Nano-Al Formed by Phase Separation in the $Al_{85}Ni_{10}Ce_5$ Metallic Glass

S.H. Wang*, Q.D. Wang and W. Wang

Hebei University of Engineering, Handan 056038, China

Abstract: A nucleation-growth control for $Al_{85}Ni_{10}Ce_5$ glass has transformed to a growth control for $Al_{83}Ni_{10}Ce_5Si_2$ glass. That's to say a small quantity of Si addition can successfully separate the Al phase to single precipitate from a eutectic precipitation composited of Al and other intermetallic compound to synthesize nanostructured materials, characteristic of microstructures with finely dispersed nanoccrystalline Al in an amorphous matrix. Favorably , no evident decrease of glass forming ability is observed in the transformation. We suggest that the Si atoms solve into Al lattice to sever as pre-exist nucleus for fcc-Al, in the same time; a nucleation reaction of fcc-Al is accompanied to compensate the nucleation rate.

Keywords: Metallic glass, differential scanning calorimetry (DSC), crystallization.

INTRODUCTION

Al-rich metallic glasses, containing transition metal (TM) and rare earth (RE) elements have attracted considerable attentions due to the occurrence of primary crystallization reaction that yields a microstructure with Al nanocrystals dispersion-embedded in an amorphous matrix, which can deserve excellent mechanical properties [1-5]. These excellent mechanical properties make this family of Al-based amorphous alloys promising candidates as advanced engineering materials. $Al_{90-x}Ni_{10}Ce_x$ amorphous alloy developed by Inoue *et al.* [6] suggest that if Ce concentration is 3 at%, then ultra fine particles (about 10nm in diameter) of fcc-Al are dispersed homogeneously in the amorphous matrix after annealing a melt quenched ribbon at appropriate temperatures. When Ce concentration exceeds 3 at%, e.g., x=5, precipitation of fcc-Al and Al-based compounds are formed simultaneously and nanocrystalline fcc-Al can not be formed. They also suggested that a slight change in Ce concentration produce a transformation from a nucleation and growth process to a grain growth process. While, the rare earth (Ce) plays an important role in promoting glass formation with a critical content of 3 at. % in the Al-Ni-Ce system [7]. Here, an attractive issue arises, how to provide a primary crystallization without decreasing the glass forming ability (namely, decreasing the Ce concentration) in Al based amorphous system. To resolve this question, more intensive investigations need to focus on the crystalline mechanism transformation from eutectic crystallization to primary crystallization. In this work, we prepared an amorphous $Al_{83}Ni_{10}Ce_5Si_2$ (with no change of Ce concentration compared to $Al_{85}Ni_{10}Ce_5$ alloy) and observed the precipitation of nanoscale fcc-Al phase by annealing the sample through a primary crystallization. The eutectic crystallization behavior of an amorphous $Al_{85}Ni_{10}Ce_5$ was also examined for comparison. The small Si addition is found to play important role in the evolution of the nanocrystalline microstructure.

*Address correspondence to these authors at the Hebei University of Engineering, Handan 056038, China; Tel: +86-310-8579535; Fax: +86-310-8579556; E-mail: shenghaiw@163.com

EXPERIMENTAL

Ingots, with nominal composition $Al_{83}Ni_{10}Ce_5Si_2$, were prepared by arc melting a mixture of pure Al (99.99 wt. %), Ni (99.97wt. %), Ce (99.96 wt. %) and Si (99.97 wt. %) in a purified argon atmosphere. Amorphous ribbons of thickness about 30 um and width about 2 mm were prepared from the master alloy ingots by a single roller melting-spinning apparatus. The precipitated phases at different temperature were assessed by XRD (D/max-rB) using Cu K_α radiation. The thermal properties were characterized by using a differential scanning calriometry (Netzsch DSC 404). High resolution transmission electron microscopy (HRTEM) observations were performed on a TECNAL 20U-TWIN.

RESULT AND DISCUSSION

Three exothermic peaks are observed in the $Al_{83}Ni_{10}Ce_5Si_2$ glass during continuous heating in DSC (Fig. **1**), no obvious glass transition observed comparing to $Al_{85}Ni_{10}Ce_5$ glass. The crystallization onset temperature (T_x) are 514 K and 538 K for $Al_{83}Ni_{10}Ce_5Si_2$ and $Al_{85}Ni_{10}Ce_5$ glasses, respectively. Both of the two glasses begin to melt at the temperature of 886 K (T_m, not shown). So, we evaluate the glass forming ability based on the T_x/T_m. The calculated results of T_x/T_m are 0.58 and 0.61 for $Al_{83}Ni_{10}Ce_5Si_2$ and $Al_{85}Ni_{10}Ce_5$ glasses, respectively. It is obviously that no evident decrease of glass forming ability is observed with a small Si addition.

To verify the origin of exothermic peaks in the DSC curve of $Al_{83}Ni_{10}Ce_5Si_2$ metallic glass, XRD experiments were performed at three different temperatures: first temperature was heated (at a rate of 10K/min) to 543 K (first peak) and then to the temperature of 603 K (second peak), and last one to 720 K (completed the third peak). Fig. (**2**) shows the XRD patterns of ribbons continuously heated to above temperatures. Formation of the fcc-Al was observed in the first stage crystallization. The second crystallization reaction is due to precipitations of Al_3Ni and intermediate metastable phase. Then, the metastable phase gradually decomposed and Al_4Ce phase formed upon the third peak. After completion of all phase transformation, the final

1874-088X/11

structure consisted of fcc- Al, Al_3Ni, Al_4Ce and some unknown phase. Here, it is of importance to note that no diffraction peak about Si or Si compounds was found in the whole devitrification process. As has been introduced above [6], precipitation of fcc-Al and Al-based compounds are formed simultaneously for $Al_{85}Ni_{10}Ce_5$ glass.

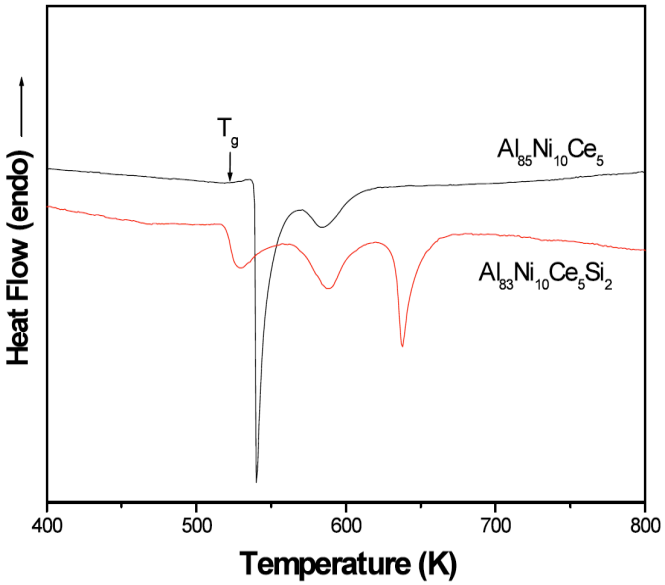

Fig. (1). Continuous heating DSC curves of the $Al_{85}Ni_{10}Ce_5$ and $Al_{83}Ni_{10}Si_2Ce_5$ glasses with a heating rate of 10K/min.

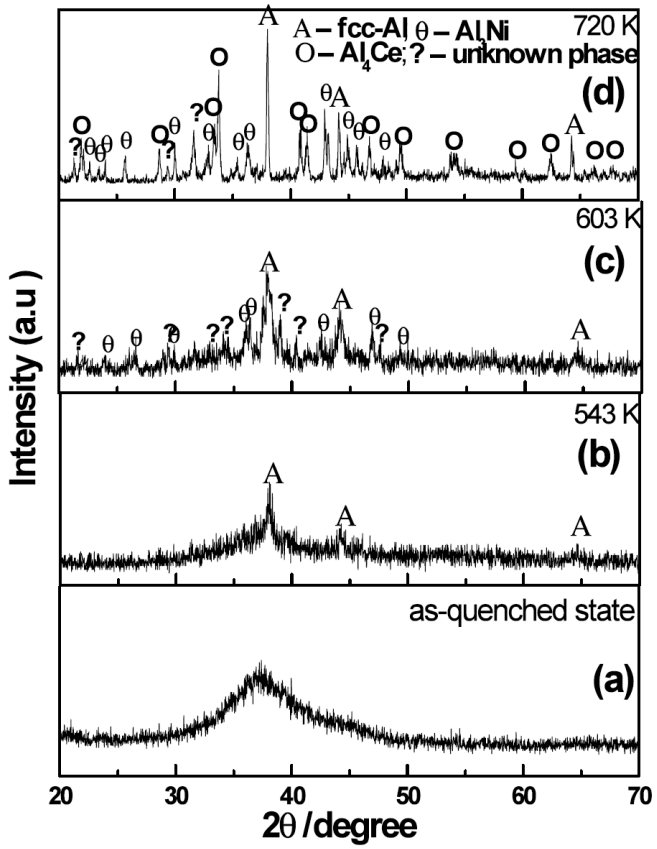

Fig. (2). X-ray diffraction patterns of the $Al_{83}Ni_{10}Ce_5Si_2$ metallic glass heating up different temperatures: (**a**) as-quenched, (**b**) 543K, (c) 603K and (**d**) 720K. (**b**), (**c**) and (**d**) corresponds to the first, second, third exothermic peak in the DSC curve, respectively.

To further study the first crystallization reaction in $Al_{83}Ni_{10}Ce_5Si_2$ glass, HREM measurements were performed, as shown in Fig. (**3**) (as-quenched (Fig. **3a**) and annealed states through the first thermal peak (Fig. **3b**, **c**). The high-resolution image of the as-quenched specimen displays a typical maze-like pattern, which is expected from the amorphous structure. The image of the annealing time for 30 s (Fig. **3b**) shows fine crystalline particles with a diameter of about 3-5 nm surrounded by the residual amorphous phase. In order to analysis the crystalline structure, a Fourier transformed pattern according to the pane in the picture is performed [the inset (A) and (B) in Fig. (**3b**)], which can get a clearer image of the lattice arrangement by eliminate the noise of the experiment equipment. Based on the transformed patterns, the crystalline phase is indexed by the structure of fcc-Al. With increasing the annealing time, the fcc-Al phase indexed by the Fourier transformed pattern grows to larger size about 10-15 nm. This is consistent with the previous results suggested by Nakazato *et al.* [8], the fcc-particles with an average size of about 15 nm homogeneously precipitated in the amorphous matrix in primary crystallization.

In an isothermal scan, a thermal signal that exhibited a monotonical decrease with time has been characteristic of a grain growth process by Chen and Spaepen in a sputtered AlMn alloy [9, 10]. Isothermal DSC scans of $Al_{85}Ni_{10}Ce_5$ and $Al_{83}Ni_{10}Ce_5Si_2$ glasses were examined for comparison as shown in Fig. (**4**). A monotonical decrease signal was observed for $Al_{83}Ni_{10}Si_2Ce_5$ glasses characteristic of grain growth, which is qualitatively different from the nucleation and growth signal observed in the $Al_{85}Ni_{10}Ce_5$ glass. The present isothermal result of $Al_{83}Ni_{10}Ce_5Si_2$ glass, in contrast to earlier studies claiming only grain growth with zero nucleation rates in some Al-rich glasses [8], exhibits a little difference. As shown in Fig. (**3**, the inset), a minor increase signal was observed in the initial time. In this case, we regard it as a small nucleation reaction (nucleation for fcc-Al).

Table 1. Lattice Spacing (d Value, 10^{-10}m) of fcc-Al (Statistical Error of the Measurement About ± 0.002 10^{-10} m)

Crystal Plane Index	(111)	(200)	(220)
Al (Standard Ref)	2.33	2.02	1.43
$Al_{85}Ni_{10}Ce_5$	2.356	2.036	1.442
$Al_{83}Ni_{10}Ce_5Si_2$	2.366	2.049	1.448

Ref: Hanawalt *et al*., Anan. Chem., 10, 475, (1938).

To summarize the DSC, XRD and HREM results, we can conclude that the small addition of Si plays an important role in the crystallization mechanism transformation, from a nucleation and growth control pattern to a growth control pattern. This transformation can deserve microstructures with finely dispersed nanocrystalline Al in an amorphous matrix, excepted excellent mechanical properties like some reported amorphous alloy [3-5]. Many researchers have proposed different option on the crystallization process. For example, Chen *et al*. [11, 12] suggested that the local atomic rearrangement instead of the long-range atomic is responsible for the formation of Al nanocrystalls during

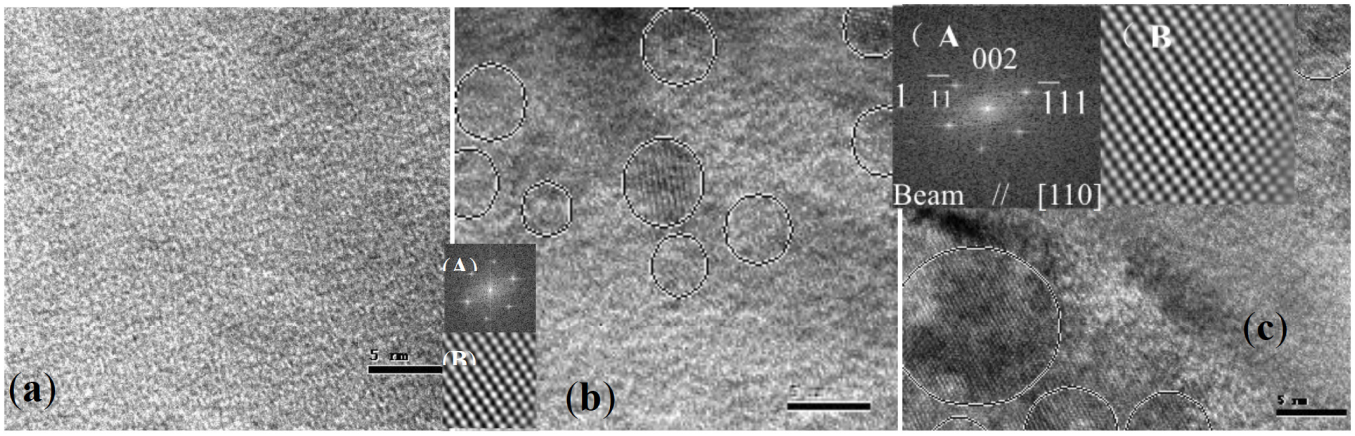

Fig. (3). HREM images of (**a**) the as-quenched specimen, (**b**) the specimen annealed at 520 K for 30 s and (**c**) increasing the annealing time to 2 min for the $Al_{83}Ni_{10}Ce_5Si_2$ alloy.

deformation, while Ye and Lu suggested a diffusion controlled primary reaction for Al precipitation [13]. Gangopadhyay [14] further investigated the crystallization processes and found that the crystallization products depend on the radius of rare earth atoms in Al-based amorphous system. While, how does the Si act in the crystallization process? In order to make it clear, we examined the lattice parameter (d value) of fcc-Al in different composition glass in the same experimental conditions for comparison, listed in Table 1. It is general known that the d value is a little larger in the alloy than in pure Al due to the lattice aberrance induced by solutes solution, exemplified by the comparison of pure Al and $Al_{85}Ni_{10}Ce_5$ glass. The d value of fcc-Al is a little larger in $Al_{83}Ni_{10}Ce_5Si_2$ glass than in $Al_{85}Ni_{10}Ce_5$ glass, combining no diffraction peaks for Si or Si compounds in the XRD pattern. Thus, we conclude that the Si atoms solve into the Al crystal lattice and the configurative character is retained during rapid quenching. The solute Si atoms may cause lattice aberrance and induce the areas soluble Si to possess higher interface energy. Here, it should be note that there are no accounts about the effect of Ni or Ce atoms solution because of no change of them in composition between the two glasses.

Crystallization of an amorphous alloy is normally regarded as a process proceeding nucleation and subsequent growth of crystals. The isothermal scan of $Al_{83}Ni_{10}Ce_5Si_2$ glass provides a monotonical decrease signal indicating a grain growth process without the corresponding nucleation process. Thus, we presume that the areas soluble Si atoms can sever as pre-exist nucleus for fcc-Al (can not detected by HREM) due to their higher interface energy caused by the lattice aberrance. Whereas, these nucleation rate is not high enough for the nucleation density to manage growth process [1], ascribed to the low Si concentration. Therefore, a nucleation reaction of fcc-Al occurs firstly to compensate the nucleation density, reflected by the minor increasing signal in the initial time in the isothermal scan. Then, a grain growth process of fcc-Al take place to form a microstructure of nanometer-sized Al crystals embedded in the amorphous matrix, as shown in Fig (**3b**, **c**). On the other hand, the glass forming ability based on T_x/T_m decreases slightly in the transformation of the crystallization mechanism, which should be an attractive property for engineering application.

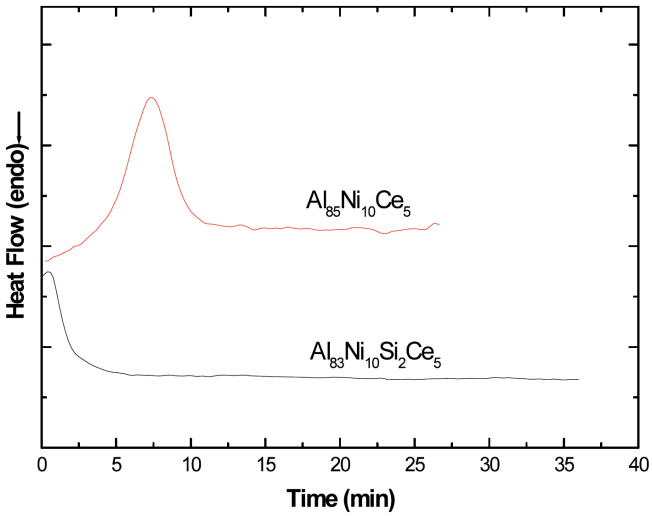

Fig. (4). Isothermal DSC scans of $Al_{85}Ni_{10}Ce_5$ and $Al_{83}Ni_{10}Si_2Ce_5$ glasses. Annealing temperature (approached at 10 K/min) is 10 K prior to crystallization onset (which was measured at10K/min as well). The inset shows the enlarged primal signal of $Al_{83}Ni_{10}Si_2Ce_5$ glass.

CONCLUSION

In summary, the crystallization processes of $Al_{83}Ni_{10}Ce_5Si_2$ and $Al_{85}Ni_{10}Ce_5$ amorphous alloys have been intensive investigated. It is found that a small Si addition can affect the crystallization behavior by promoting the formation of nanoscale fcc-Al phase in an amorphous matrix, which is expected for an excellent mechanical property. This result is contributed to the Si action in the crystallization process. The areas soluble Si atoms due to lattice aberrance are estimated to sever as pre-exist nucleus for fcc-Al to accelerate a primary crystallization, in the same time, a nucleation reaction of fcc-Al is accompanied to compensate the nucleation rate. In addition, no evident decrease of glass forming ability is observed in this transformation.

ACKNOWLEDGEMENT

This work has been supported by the Science Foundation of Hebei (project Number. 09395113D).

REFERENCE

[1] Wu RI, Wilde G, Perepezko JH. Glass formation and primary nanocrystallization in Al-base metallic glasses. Mater Sci Eng A 2001; 301: 12-17; Foley JC, Allen DR, Perepezko JH. Strategies for the development of nanocrystalline materials through devitrification. Mater Sci Eng A 1997; 226–228: 569-73.

[2] Chen H, He Y, Shiflet GJ. Mechanical properties of partially crystallized aluminum based metallic glasses. Scr Metall Mater 1991; 25: 1421-4.

[3] Allen DR, Foley JC, Perepezko JH. Nanocrystal development during primary crystallization of amorphous alloys. Acta Mater 1998; 46: 431-40.

[4] Bian XF, Sun BA, Hu LN. Medium-Range Order Structure and Fragility of Superheated Melts of Amorphous CuHf Alloys. Chin Phys Lett 2006; 23: 1864-7.

[5] Inoue A. Amorphous, nanoquasicrystalline and nanocrystalline alloys in Al-based systems. Prog Mater Sci 1998; 43: 365-520.

[6] Tsai AP, Kamiyama T, Kawamura Y. Formation and precipitation mechanism of nanoscale Al particles in Al-Ni base amorphous alloys. Acta Mater 1997; 45: 1477-87.

[7] Inoue A, Nakazato K, Kawamura Y. The effect of Cu addition on the structure and mechanical properties of Al-Ni-M (M Ce or Nd) amorphous alloys containing nanoscale fcc-Al particles. Mater Sci Eng A 1994; 179-180: 654-8.

[8] Nakazato K, Kawamura Y, Tsai AP. On the growth of nanocrystalline grains in an aluminum-based amorphous alloy. Appl Phys Lett 1993; 63: 2644-6.

[9] Chen LC, Spaepen F. Grain growth in microcrystalline materials studied by calorimetry. Nanostructured Materials 1992; 1: 59-64.

[10] Chen LC, Spaepen. The configurational entropy of two-dimensional random Penrose tilings. Mater Sci Eng 1988; 99: 339-43.

[11] Chen H, He Y, Shiflet GJ. Mechanical properties of partially crystallized aluminum based metallic glasses. Scr Metall Mater 1991; 25: 1421-4.

[12] Gao MC, Shiflet GJ. Devitrification sequence map in the glass forming Al–Ni–Gd system. Scrip Mater 2005; 53: 1129-34.

[13] Ye F, Lu K. Crystallization kinetics of Al–La–Ni amorphous alloy. J Non-Cryst Solids 2000; 262: 228-35.

[14] Gangopadhyay AK, Croat TK, Kelton KF. The effect of phase separation on subsequent crystallization in Al88Gd6La2Ni4. Acta Mater 2000; 48: 4035-43.

Received: August 28, 2010 Revised: November 26, 2010 Accepted: December 22, 2010